学位論文

A morphological study of postoperative adhesions between injured tissue and intact peritoneum in the rat liver

（ラット肝臓の損傷された組織と正常な腹膜の間に形成される術後癒着に関する形態学的研究）

旭川医科大学大学院医学系研究科博士課程医学専攻

鈴木　達也

（河野　透、暮地本　宙己、平　義樹、渡部　剛、古川　博之）

Postoperative adhesion formation is one of the major clinical problems that should be addressed. Postoperative adhesions after abdominopelvic surgery cause small-bowel obstruction and female infertility, and the large impact of adhesion-related morbidity on human health and healthcare costs emphasizes the need to develop prophylactic strategies.[1] Although various prophylactic agents have been developed and shown to be effective in adhesion prevention, limited clinical trials have shown efficacy in reduction of adhesion-related morbidity.[2,3] In addition to assessing the clinical efficacy of the available agents and developing new agents, a better understanding of the pathophysiology of adhesion formation is essential to improving prophylactic strategies.

The pathophysiology of adhesion formation has been extensively studied but remains to be clarified. The process of adhesion formation is briefly described as follows: tissue injury involving the peritoneum causes inflammation and fibrin deposition, which connects the injured tissue to the tissue of an opposing organ. If the fibrin persists due to suppressed fibrinolysis, tissue repair extends into the fibrin scaffolding, leading to scar formation.[3,4,5] The mechanisms of the fibrinous

connection of tissues, such as inflammation and fibrinolysis, have been examined in detail.[6,7,8,9] However, the role of the peritoneum in adhesion formation has not been well studied.

The peritoneum may act as a protective epithelium against adhesion formation, as suggested by the fact that the peritoneum consists of mesothelial cells (MCs) and a basement membrane (BM) and displays epithelial characteristics.[10] Schade and Williamson noted that detachment of MCs appeared to be the critical event in an experimental adhesion model.[11] Moreover, Lamont et al. and Haney and Doty showed that adhesions more frequently formed when two opposing peritoneums were injured than when only one peritoneum was injured while the opposite peritoneum was left intact.[12,13] These studies suggest that adhesions form only after both of the two opposing peritoneums lose their epithelial function.

Little is known, however, about how an injured tissue affects the opposite intact peritoneum when these tissues are approximated. Only one side of the two opposing peritoneums is intentionally injured in many experimental adhesion

models,[6,7,8] which implies that adhesions form when an injured tissue and the opposite intact peritoneum are approximated. Hence, we hypothesized that an injured tissue would deprive the opposite intact peritoneum of its epithelial function and form adhesions with the opposite intact tissue.

In this study, we performed a histological examination of a hepatic model of adhesions between injured and intact lobes to clarify how an injured tissue affects the opposite intact peritoneum during adhesion formation.

MATERIALS AND METHODS

Animals

In total, 91 male Sprague-Dawley rats weighing between 300 and 380 g (Charles River Laboratories, Yokohama, Japan) were used. The animals were housed at a constant room temperature with 12-hour light and dark cycles and

were provided standard rodent chow and water ad libitum. The research protocol was approved by the institutional animal care and use committee of Asahikawa Medical University. All animal procedures were in accordance with the Guide for the Care and Use of Laboratory Animals (National Research Council of the National Academies).

Hepatic model of adhesion formation between injured tissue and opposite intact peritoneum

The medial lobe of the rat liver consists of two portions: the right medial lobe (RML) and the left medial lobe (LML).[14] Adhesions were induced between the RML and the LML, where the two peritoneums are located face to face in the main fissure.

Surgery was performed in an aseptic environment. Rats were anesthetized with diethyl ether. After the skin was shaved and cleansed with 70% ethanol, the abdomen was opened through a 5-cm upper midline incision. The xiphoid process was grasped and lifted with a hemostat. The falciform ligament was cut,

and two pieces of wet absorbent cotton were inserted beneath the diaphragm to push the liver caudally. The RML was raised with a wet cotton swab, and the exposed medial aspect of the LML was cauterized using bipolar electrocautery forceps (N1-14, Senko Medical Instrument, Tokyo, Japan) by tracing a 1-cm line for 2 seconds (Figures 1a and b). The inner width of the forceps tip was adjusted to 1 mm under a stereomicroscope, and the output of electrocautery (MS-7000E, Senko Medical Instrument) was set at 6 on the dial, which corresponded to 15 watts when measured by an electrosurgery analyzer (RF303, BIO-TEK, Winooski, VT, USA). Physiological saline was dripped onto the cauterized surface to maintain moisture. The medial aspect of the RML, which was opposite to the cauterized aspect of the LML, was grossly observed immediately after cauterization. Occasionally, a flash occurred at the instant of cauterization, and the peritoneum of the RML turned slightly red, indicating an accidental injury of the RML. In such cases, the animals were excluded from the study. The rectus sheath was closed by interrupted sutures, and the skin was closed continuously

with 3-0 silk threads. Saline was often dripped onto the liver surfaces to maintain moisture during surgery.

Relaparotomies were performed at 1, 6, 24, and 48 hours and at 4 and 8 days after cauterization (n=12 at each time point). As controls, samples were taken from the following groups: normal rats (n=9); rats immediately after cauterization (n=4); and rats 6 and 24 hours and 4 days after sham operation in which the same procedures were performed except liver cauterization (n=2 at 6 hours and, n=3 at 24 hours and 4 days). The livers were excised and processed for histological examination.

Preparation for light microscopy

During the relaparotomies, the rats were anesthetized with ether and perfused with 20 mL of bicarbonate Ringer's solution containing 10 U/mL heparin, followed by 200 mL of phosphate buffered saline (PBS) containing 4% paraformaldehyde at a flow rate of 10 mL per minute (n=6 at each time point after cauterization, n=4 immediately after cauterization, and n=3 for normal rats

and 24 hours and 4 days after sham operation). The medial lobe, containing the RML and LML, was excised en bloc and immersed in the fixative at 4°C overnight.

The RML and LML were cut together in a plain perpendicular to the cauterized line, near the middle of the line (Figures 1b and c). One half of the divided tissue containing the domed portion of the medial lobe was dehydrated in ethanol, substituted with chloroform, and embedded in paraffin. The other half of the divided tissue, containing the sharper edges of the RML and LML, was immersed in PBS containing 30% (w/w) sucrose at 4°C overnight and embedded in OCT compound (Sakura Finetek, Tokyo, Japan) using liquid nitrogen.

Next, 5-μm paraffin sections were prepared on a microtome and stained with hematoxylin and eosin (HE). The sections were also examined by phosphotungstic acid hematoxylin staining for the identification of fibrin and Sirius red and Fast Green staining for collagen. Paraffin sections were used for routine observation and cell counting by immunohistochemical analysis. 8-μm

frozen sections were cut on a cryostat and immunostained and are presented in the figures.

Preparation for transmission electron microscopy (TEM)

Rats were anesthetized with ether and perfused with the Ringer's solution, followed by 200 mL of 0.1 M phosphate buffer (PB) containing 2% glutaraldehyde and 2% paraformaldehyde (n=3 for normal rats and at each time point after cauterization). The medial lobe was excised en bloc and immersed in the fixative at 4°C overnight.

The RML and LML were cut together in few-millimeter slices perpendicular to the cauterized line, fixed in 0.1 M PB containing 1% osmium tetroxide (Merck) for 2 hours at 4°C, dehydrated in ethanol, substituted with propylene oxide, and embedded in epoxy resin (Epon 812 Resin Embedding Kit, TAAB Laboratories Equipment, Berkshire, UK).

Next, 0.5-μm semithin sections were stained with toluidine blue and examined with an optical microscope. 0.1-μm ultrathin sections were stained with lead

citrate and uranyl acetate and examined with a transmission electron microscope (H-7650, HITACHI, Tokyo, Japan).

Preparation for scanning electron microscopy (SEM)

Rats were anesthetized with ether and perfused with the Ringer's solution, followed by 200 mL of 0.1 M PB containing 2% glutaraldehyde (n=3 for normal rats and at each time point after cautery, and n=2 for 6 hours after sham operations). The medial lobe was excised en bloc and immersed in the fixative at 4°C overnight.

When the RML and LML were adherent over a broad area, it was difficult to observe the peritoneums in or adjacent to the adherent area. Therefore, specimens in which the two lobes were separate or loosely attached in a focal area were used for observation. The two lobes were cut apart at the domed portion of the medial lobe. When a focal and loose adhesion was present, an invisible line connecting the two lobes was cut with fine scissors. The tissues were incubated in 0.1 M PB containing 2% tannic acid for 3 hours at room

temperature, shaded from the light. After washed, the tissues were incubated in 0.1 M PB containing 1% osmium tetroxide for 2 hours at room temperature, dehydrated in ethanol, substituted with 3-methylbutyl acetate, and dried in a critical point dryer (HCP-2, HITACHI) using liquid carbon dioxide. The tissues were mounted on an aluminum specimen mount (Okenshoji, Tokyo, Japan), coated with platinum-palladium in an Ion Sputter (E-1030, HITACHI), and examined with a scanning electron microscope (S-4100, HITACHI).

Immunohistochemistry

When antigen retrieval was needed, paraffin-embedded or frozen sections were incubated in 200 mL of pure water containing 0.05% citraconic anhydride (Immunosaver, Nissin EM, Tokyo, Japan) at 95°C for 10 or 45 minutes using a hot water dispenser.[15] The sections were blocked with normal horse serum and incubated with primary antibodies overnight at room temperature. The sections were then incubated with secondary antibodies labeled with Alexa Fluor 488 or 594 (A11029, A11032, A11034, A11037, A11055, and A21207; Life

Technologies, Tokyo, Japan) for 1 hour at room temperature. The nuclei were stained with DAPI, and the sections were examined with an optical fluorescence microscope (BX60, Olympus, Tokyo, Japan).

The following primary antibodies were used: anti-keratin (clone C-11, BM555, Acris Antibodies, Herford, Germany), anti-ZO-1 (rabbit immunoglobulin [Ig], 61-7300, Life Technologies), anti-laminin (rabbit Ig, L9393, Sigma-Aldrich, Tokyo, Japan), anti-laminin γ1 (clone D18, sc-59846, Santa Cruz Biotechnology, Santa Cruz, CA, USA), anti-elastin (rabbit Ig, AB2039, Merck Millipore, Billerica, MA, USA), anti-CD68 (clone ED1, MCA341, AbD Serotec, Bio-Rad Laboratories, Raleigh, NC, USA), anti-α-smooth muscle actin (α-SMA) (clone 1A4, M0851, Dako, Tokyo, Japan), and anti-fibrinogen/fibrin (goat IgG, 55731, MP Biomedicals, Tokyo, Japan).

Measurement of the adherent area

The adherent area was measured in paraffin sections stained with HE. The cauterized lobe, i.e. the LML, was positioned downward in the microscopic field,

and the opposite lobe, i.e. the RML, was positioned upward, so that the peritoneums were horizontal (Figure 1d). Micrographs were sequentially taken throughout the cauterized area with a ×20 objective lens and were divided by vertical lines into 100-μm-wide sequential segments, which were numbered from left to right in the cauterized area (Figure 1d). The segments in which the two lobes were adherent and the segments in which cauterized hepatocytes were necrotic were counted.

Counts of MCs and segments in which MCs were absent or discontinuous

MCs were labeled in paraffin sections immunostained for keratin and ZO-1. The two lobes were positioned as described above, and sequential micrographs were taken with a ×40 objective lens, divided into segments, and numbered similarly. The nuclei of the MCs in each lobe or in the adherent area were counted in each segment (Figures 3a and b), and histograms of the counts of nuclei per segment were prepared for all specimens until 24 hours after cauterization or sham operation, to express the distribution of MCs.

In the same sections, the segments in which the MCs of the opposite lobe were absent or discontinuous were counted to evaluate the reduction in the number of MCs in the opposite lobe.

In addition, isolated MCs were occasionally observed in the segments in which the MCs of the opposite lobe were discontinuous or in which adhesion was present (Figure 3b). The nuclei of the isolated MCs in each lobe or in the adherent area were counted in each segment, and all of the counts of nuclei per segment in the two lobes and in the adherent area were added together to calculate the total count of nuclei in the entire section.

Count of CD68-positive cells

Monocytes/macrophages were labeled in paraffin sections immunostained for CD68. Laminin was stained at the same time to locate the BM of the opposite peritoneum. The two lobes were positioned as described above, and sequential micrographs were taken, divided into segments, and numbered similarly. The nuclei of CD68-positive cells and of total cells were counted in each segment.

Cells were counted in the area between the necrotic hepatocytes of the cauterized lobe and the intact hepatocytes of the opposite lobe in the segments in which adhesions were present or between hepatocytes and the peritoneal cavity in the segments in which adhesions were not present. In addition, nuclei were counted separately on each side of the BM of the opposite peritoneum, i.e. on the cauterized side and on the opposite side (Figure 9c). The sides of the BM of the cauterized peritoneum could not be distinguished because the BM disappeared in the central part of the cauterized area. Histograms of the counts of nuclei per segment were prepared from all specimens until 48 hours after cauterization or 24 hours after sham operation.

To characterize cell accumulation in the adherent area, four specimens in which the adherent areas were larger than in the other two specimens were selected at each time point after cauterization. The average count of nuclei per segment was calculated in the cauterized area to express the extent of cell accumulation.

Statistics

Values are expressed as the mean ± s.d. The significance of differences between 24 hours after cauterization and 24 hours after sham operation was determined by Mann-Whitney's U test or a two-sample t test with Welch's correction using Microsoft Excel (Microsoft Corporation, Redmond, WA, USA).

RESULTS

Adhesions form between a cauterized lobe and the opposite intact lobe of the rat liver

By HE staining, we observed that adhesions formed when a cauterized lobe and the opposite intact lobe were approximated. In this model, the cauterized tissue was severely injured, as indicated by the extensive necrosis of cauterized hepatocytes (Figure 1d), measuring 3833 ± 520 μm in width and 1617 ± 279 μm

in depth at 24 hours (n=6), and tissue deformation in the central part of the cauterized area. In contrast, the hepatocytes of the opposite lobe were intact in most of the area, except that focal necrosis was occasionally observed at 24 hours. Adhesions formed over the necrotic tissue (Figure 1d). Inflammation was conspicuous at 24 hours, and tissue repair was proceeding at 4 days (Figures 1e and f). The adherent area enlarged until 24 hours and did not change afterward, whereas adhesions were occasionally absent at 48 hours and later (Figure 1g). The necrotic area diminished at 8 days as tissue repair progressed.

All animals survived the surgery. Of 12 animals at each time point, including animals examined by electron microscopy, the incidence of adhesions, as assessed by gross and histological findings, was as follows: n=0 at 1 hour, n=8 at 6 hours, n=12 at 24 hours, n=9 at 48 hours, n=7 at 4 days, and n=9 at 8 days. No adhesions were present after sham operation (n=3 at 24 hours and 4 days). These observations indicated that adhesions could form after approximation of a cauterized lobe and the opposite intact lobe. The findings described hereafter will pertain to adherent specimens at 48 hours after cauterization and later.

The normal liver peritoneum is an epithelial tissue consisting of MCs and a BM

Examination of the normal liver peritoneum showed that this tissue possessed typical epithelial characteristics (Figure 2). Normal MCs had numerous microvilli, were present on the BM, and were flat and connected to each other by cell-cell junctions. The appearance of normal MCs was compared with the appearance of MCs affected by a cauterized tissue, as described below. Beneath the BM, a layer of elastic fibers was present (Figures 2b and f). The elastic fibers were thicker and more distinct than the BM and are indicated in the micrographs to show the peritoneal layer of the opposite lobe.

The peritoneum of the opposite lobe is denuded of MCs until 6 hours

We examined the early effects of a cauterized tissue on the opposite peritoneum. MCs were counted to determine their distribution and quantify their presence (Figure 3). As shown in the representative histograms, the MCs of the opposite

lobe began decreasing in number until 1 hour and disappeared in continuous segments (Figure 3c). More than half of the opposite peritoneum that came into contact with the necrotic tissue had lost MCs at 1 hour (Figure 3e). The denuded area appeared to enlarge until 6 hours and did not change at 24 hours (Figure 3e).

When observed by electron microscopy, the opposite peritoneum was denuded of MCs in a large island-shaped area at 1 hour, revealing the underlying BM (Figures 4a and b). The irregular surfaces and swollen organelles of the MCs at the margin of the denuded area indicated that these cells were severely injured (Figures 4a and b and 5a). At 6 hours, the injured MCs observed at the margin at 1 hour were rarely observed by SEM (Figures 4d and e), whereas isolated and severely injured MCs and necrotic debris were occasionally observed under the covering fibrin in the denuded area by TEM (Figures 5b and c). This finding suggested that the injured MCs at the margin were detached and more severely injured until 6 hours. In contrast, remnant MCs around the margin notably reduced the number of their microvilli until 6

hours (Figures 4a, c, d, and f), yet they possessed normal cytoplasmic organelles at 6 hours (Figure 5d), suggesting that the cells' injuries were mild and reversible. The microvilli did not decrease in number at 6 hours after sham operation.

These findings indicated that the early effects of a cauterized tissue on the opposite intact peritoneum were the detachment and injury of MCs in a large area, leading to exposure of the underlying BM. The remnant MCs around the margin, in contrast, appeared to survive.

Inflammation increases until 24 hours, and inflammatory cells appear to migrate from the opposite intact lobe to the cauterized lobe

One of the noticeable events from 6 to 24 hours was infiltration of inflammatory cells into the adherent area. Monocytes/macrophages appeared not only on the cauterized lobe but also in the subserosa of the opposite lobe until 6 hours (Figures 6a and b). The presence of monocytes/macrophages in the subserosa of the opposite lobe suggested that chemotaxis occurred through the peritoneal

layer of the opposite lobe after the denudation of MCs. Granulocytes, especially neutrophils, were also as conspicuous as monocytes/macrophages on the cauterized lobe and in the subserosa of the opposite lobe at 6 hours (data not shown). The accumulation of monocytes/macrophages increased until 24 hours (Figure 6c). The absence of monocytes/macrophages in the subserosa of the opposite lobe at 24 hours after sham operation indicated that the migration was caused by the approximation of the cauterized tissue itself, and not by the surgical procedures other than electrocauterization (Figure 6d).

As shown in the representative histograms at 24 hours, monocytes/macrophages were present throughout the cauterized area on either side of the BM of the opposite peritoneum (Figure 6e). Monocytes/macrophages were shown to increase in number until 24 hours and were the majority of infiltrating cells at 24 hours (Figure 6f). These findings indicated that inflammation was most conspicuous at 24 hours and suggested that the cauterized tissue caused the chemotaxis of inflammatory cells from the opposite lobe to the cauterized lobe.

Fibrin increases for 24 hours and attaches to exposed BM

Another marked event that occurred until 24 hours after the procedure was increasing deposition of fibrin. As observed by SEM, the fibrin covering the denuded peritoneum increased from 1 hour to 6 hours (Figures 4a, b, d, and e). Observation by immunohistochemistry showed that fibrin was extensively present in the adherent area between the cauterized tissue and the BM of the opposite peritoneum at 24 hours (Figure 7a). In addition, observation by TEM confirmed that fibrin had attached to the exposed BM of the opposite peritoneum at 24 hours (Figure 7b). These observations showed that the increasing fibrin that was deposited in the adherent area connected the two lobes over a broader area until 24 hours via the attachment of fibrin to the exposed BM of the opposite peritoneum.

Remnant MCs in the opposite lobe undergo morphological changes for 24 hours after electrocauterization

It has been shown so far that the opposite peritoneum was denuded of MCs until 6 hours and that inflammation and fibrin deposition increased until 24 hours after cauterization. We then further examined how the remnant MCs of the opposite lobe were affected by a cauterized tissue from 6 to 24 hours.

Immunohistochemical staining for keratin and ZO-1 showed that there were isolated MCs present in the adherent area at 24 hours (Figure 3b). There appeared to be more isolated MCs in the peripheral part of the adherent area than in the central part (Figure 3d, gray bars). Isolated MCs were sparse in the adherent area; the averages of the counts of nuclei per segment in the adherent area were 0.78 ± 0.45 at 24 hours as to isolated MCs (n=6). Nonetheless, isolated MCs obviously increased in number until 24 hours (Figure 3f).

Observation by TEM revealed isolated MCs in an arched or saccular shape resting on the BM of the opposite peritoneum in the adherent area at 24 hours (Figure 8). The cells were identified as MCs by their microvilli, which closely resembled those of normal MCs (Figures 8b and e, see also 2e). The arched MCs appeared to be in the process of forming a saccular shape (Figures 8a and

b). The saccular MCs were usually located on the BM of the opposite peritoneum (Figure 8c), indicating that these cells had originated from the opposite peritoneum. The saccular MCs were occasionally located away from the BM (data not shown). Whereas several of the saccular MCs consisted of two MCs (Figures 8c-e), others appeared to have been formed by a single MC (Supplementary Figure 1). Fibrin was nearly invariably observed in close proximity to the outer rims of the arched and saccular MCs (Figures 7b and e), suggesting the involvement of fibrin in the saccular changes in MCs. Fibrin often attached to the exposed BM near the saccular MCs (Supplementary Figures 1e and f).

Observation by TEM revealed another type of morphological change at 24 hours. There were isolated and tall MCs in the adherent area at 24 hours (Figure 9). These cells were also identified as MCs by their microvilli, which closely resembled those of normal MCs (Figures 9c and g, see also 2e). Whereas several of these cells were located on the BM of the opposite peritoneum (Figures 8a-d), others were located away from the BM and on fibrin (Figure 8e-g),

suggesting that the isolated and tall MCs on the opposite lobe had detached from the BM and were migrating into the adherent area. The isolated and tall MCs were occasionally located on the BM of the opposite peritoneum and on fibrin at the same time (Supplementary Figure 2), and these MCs appeared to be in the process of detaching from the BM. The isolated and tall MCs at 24 hours were presumed to originate from the opposite peritoneum because these cells often rested on that peritoneum's BM, whereas several of the cells appeared to have originated from the peritoneal margin of the cauterized lobe.

These observations showed that the remnant MCs of the opposite peritoneum underwent two types of morphological changes in the adherent area until 24 hours after the procedure. We then observed how these affected MCs behaved afterward.

Whereas several isolated MCs are still present in the adherent area at 48 hours and later, tall MCs regenerate the peritoneum on the marginal surfaces of the adherent area

Saccular MCs were present in the adherent area even at 48 hours and later. At 48 hours, there were two types of saccular MCs, i.e. those with very thin cytoplasm and scarce cytoplasmic organelles and those with thick cytoplasm and relatively abundant organelles. At 4 days, only saccular MCs with thin cytoplasm were observed (data not shown).

In contrast, isolated and tall MCs were not observed inside the adherent area at 48 hours and later. Instead, relatively tall MCs were observed on the marginal surfaces of the adherent fibrin scaffolding and mostly formed cell-cell junctions with each other. This observation suggested that several of the isolated and tall MCs that had been observed at 24 hours participated in regeneration on the marginal surfaces. At 4 days, taller MCs with abundant cytoplasmic organelles nearly covered the marginal surfaces, forming a continuous peritoneum (data not shown).

Tissue repair occurs between the cauterized lobe and the opposite intact lobe, and tissue-repairing cells appear to migrate from the opposite intact lobe to the cauterized lobe

We have shown that the MCs of the opposite lobe lost their normal epithelial morphology in the early steps of adhesion formation. Finally, we examined how a fibrous adhesion formed between a cauterized tissue and the opposite intact tissue.

Immunohistochemical staining for α-SMA showed that myofibroblasts began infiltrating into the adherent area until 48 hours and obviously increased in number at 4 days (Figures 10a-c). The accumulation of myofibroblasts in the subserosa of the opposite lobe suggested that the cells were trying to migrate from the opposite lobe to the cauterized lobe. Myofibroblasts were not present in the subserosa of the opposite lobe at 4 days after the sham operation (Figure 10d).

Collagen deposition followed the accumulation of myofibroblasts. As shown by phosphotungstic acid hematoxylin staining, Sirius red and Fast Green staining

and TEM, fibrin was replaced by collagen from 48 hours to 4 days, and scar tissue with thick collagen bundles formed until 8 days (Supplementary Figure 3).

In addition, the opposite intact tissue appeared to contribute to angiogenesis in the adherent tissue. Immunohistochemical staining for laminin-γ1 and elastin showed that the BM and elastic fibers of the opposite peritoneum were nearly continuous at 24 hours (Figure 11a). At 4 days, however, the BM of the opposite peritoneum was partly indistinct, and a newly formed BM with a lumen-like structure was observed in the adherent area (Figure 11b, upper panel). There were more gaps in the peritoneal layer of the elastic fibers at 4 days than at 24 hours (Figure 11b, middle panel), and the lumen-like BM had grown through the gaps in the elastic fibers (Figure 11b, lower panel). Observation by TEM revealed that blood vessels had grown through the gaps in the elastic fibers of the opposite peritoneum (Figure 11c) and indicated that angiogenesis occurred from the opposite lobe to the cauterized lobe.

These observations suggested that the opposite intact tissue participated in tissue repair in the adherent area during fibrous adhesion formation after a cauterized tissue and the opposite intact tissue are approximated.

DISCUSSION

This is the first study showing that a cauterized tissue causes significant structural changes in the opposite intact peritoneum and is repaired through interaction with the opposite intact tissue, resulting in the formation of a fibrous adhesion. The major structural changes are as follows: (1) the opposite peritoneum is denuded of MCs until 6 hours, exposing the underlying BM; (2) inflammation increases on either side of the BM of the opposite peritoneum until 24 hours; (3) exuded fibrin attaches to the exposed BM until 24 hours; (4) the remnant MCs of the opposite peritoneum are isolated and change their morphology into a saccular or tall shape until 24 hours; and (5) tissue repair

proceeds in the adherent area until 8 days, to which the opposite intact tissue may contribute.

The detachment and severe injury of the MCs of the opposite peritoneum until 6 hours leads to loss of the epithelial function of the peritoneum, as indicated by the observation that fibrin attaches to the exposed BM until 24 hours. In other words, exposure of the BM by the detachment of MCs allows fibrin to attach to the BM, whereas fibrin does not attach to the peritoneum as long as a continuous sheet of MCs rests on the BM. A negligible increase in the number of inflammatory cells at 1 hour indicates that these cells are not involved in the detachment of MCs at this time. The morphological findings for the opposite peritoneum at 1 hour, such as the denudation in an island-shaped area and the severe injury of MCs at the margin, suggest that the detachment and injury of MCs is caused by a mechanical force, rather than by chemical or bioactive factors. MCs have been reported to possess lubricants such as sialomucin or phosphatidylcholine on their apical surface,[16,17,18,19] and the loss of MCs from a cauterized tissue may increase friction between the cauterized tissue and the

opposite peritoneum. The accumulation of inflammatory cells associated with the enlargement of the denuded area until 6 hours suggests that inflammatory cells may be involved in further denudation. One possibility is that infiltrated neutrophils injure MCs via oxidative stress[20.21]. The early detachment of MCs is in line with observations in a hepatic model of adhesions induced by an intraperitoneal injection of silica and in a pericardial model of adhesions induced by an intrapericardial injection of bacterial toxins, in which intact peritoneums are involved.[11,22] The present study shows that an injured tissue causes the detachment of MCs from an intact peritoneum when the two tissues come into contact and indicates that the detachment of MCs may be a common step in adhesion formation when intact peritoneums are involved.

As described above, the attachment of fibrin to the exposed BM indicates the significance of the role of MCs as a protective epithelium against adhesion formation. The mechanisms by which fibrin attaches to the BM have not been documented in detail, but there are reports showing that fibrinogen binds to components of the BM.[23,24] The attachment of fibrin to the exposed BM is

consistent with the observations of Schade and Williamson and supports their view that adhesions appear to occur only when two denuded peritoneums are opposed.[11]

Whereas the effect of a cauterized tissue on the opposite intact peritoneum until 6 hours is the loss of MCs themselves, the effects until 24 hours are the morphological changes in MCs and are accompanied by an increase in inflammation, suggesting that inflammatory cytokines or exuded fibrin is involved in the cells' morphological changes.

The isolation of MCs and their morphological changes into a saccular shape appear to further contribute to the loss of the epithelial function of the opposite peritoneum. The invariable presence of fibrin in close proximity to the saccular MCs suggests that fibrin is involved in the saccular changes. One possible mechanism is that if MCs had a tendency to turn their basal surfaces toward fibrin, the MCs surrounded by fibrin might form a saccular shape. It has been shown that cultured MCs interact with fibronectin via integrin isoforms that are located at their basal surfaces.[25] In addition, the integrin isoforms that have been

shown to be located at the basal surfaces of cultured MCs might bind to fibrin directly, or indirectly via fibronectin.[25,26] However, how the polarity of MCs is affected by fibrin has been poorly characterized. The saccular changes in MCs may facilitate exposure of the underlying BM and allow fibrin to attach to the BM over a broader area. In addition, the surrounding fibrin appears to prevent the saccular MCs from making cell-cell contacts with neighboring MCs and from forming an epithelial sheet. These findings indicate that the isolation of and saccular changes in MCs augments the loss of the epithelial function of the opposite peritoneum.

However, it is difficult to determine whether the isolation of MCs and their morphological changes into a tall shape contribute to the loss of epithelial function of the opposite peritoneum. Inflammatory factors may be involved in the isolation of MCs, their morphological changes, and their detachment from the BM, as suggested by reports that inflammatory cytokines change the morphology of cultured MCs into an isolated and cuboidal shape and allow these cells to detach from the underlying matrix.[27,28] The isolated and tall MCs are

presumed to migrate on fibrin and participate in the epithelialization of the marginal surface of the adherent area at 48 hours, whereas several of the cells might be surrounded by fibrin afterward and form a saccular shape with thick cytoplasm and abundant organelles until 48 hours. In addition, MCs may change their phenotype into a mesenchymal one during tissue repair or fibrosis,[29,30] but this change could not be verified in the present study. The isolation and detachment of MCs from the BM may lead to the loss of epithelial function. However, given that the isolated and tall MCs most likely participate in the epithelialization, we did not conclude that the cells merely lose their epithelial function; if fibrin degrades and the two lobes are separated afterward, the cells might cover the surfaces of each lobe.

The present study shows that a cauterized tissue has three types of effects on the MCs of the opposite intact peritoneum. The finding that the denuded area enlarges until 6 hours and appears not to change at 24 hours indicates that the early detachment and injury of MCs contributes more to the loss of the epithelial function of the opposite peritoneum than do the later morphological changes in

MCs. In this context, the early detachment and injury of MCs need to be further studied to determine the exact mechanisms of these events and understand how to prevent them. Nonetheless, the presence of saccular and tall MCs was not negligible, but rather relatively conspicuous in the peripheral part of the adherent area when observed by TEM. The significance of these morphological changes needs to be further investigated. The effects of an injured tissue on an opposing intact peritoneum have not been well studied so far. Watters and Buck showed that peeling off MCs without damaging the underlying tissue caused an increase in the number of proliferating MCs on the apparently uninjured opposite peritoneum at 48 hours.[31] This finding suggests that the effects of an injured peritoneal site on the opposite intact peritoneum depend on the severity of the tissue injuries. Moreover, the presence of isolated MCs in a saccular or tall shape at 24 hours has not been described in several studies on mesothelial regeneration in an injured peritoneum using electron microscopy,[32,33,34,35,36] indicating that the morphological changes in MCs at 24 hours observed in the present study are distinctive changes in the opposite peritoneum and not in the

injured peritoneum.

In addition to affecting the opposite intact peritoneum, tissue cauterization has been shown to cause tissue repair, to which the opposite intact tissue may contribute. Macrophages may play a vital role in tissue repair by releasing growth factors such as TGF-β and VEGF; TGF-β induces the differentiation of myofibroblasts, and VEGF stimulates angiogenesis.[37,38,39] The significance of macrophages in adhesion formation has been shown by a report that inhibiting the chemotactic aggregation of peritoneal macrophages at the injured site prevents adhesion formation.[40] The myofibroblasts that begin accumulating until 48 hours are presumed to produce collagen at 4 days and later. Hence, the cauterized tissue causes the accumulation of monocytes/macrophages, which then facilitate tissue repair, leading to fibrous adhesions. The accumulation of the cells on the opposite side of the BM/elastic fibers of the opposite peritoneum suggests that the cauterized tissue causes chemotaxis beyond the layer of the BM/elastic fibers. It is not clear what proportion of the accumulated monocytes/macrophages or myofibroblasts on the cauterized side derives from

the opposite side, but the cells may migrate through increasing gaps in the BM/elastic fibers of the opposite peritoneum and toward the cauterized side. In contrast, the newly formed blood vessels on the cauterized side obviously derive from the opposite intact tissue. These findings suggest that the opposite intact tissue can provide the adherent and cauterized tissues with the cells that participate in tissue repair and that an intact tissue can cause adhesions when the intact tissue comes into contact with an injured tissue.

The results of the present study, which found that a cauterized tissue and an opposing intact peritoneal surface together cause fibrous adhesions, are not in line with the findings of another related study, and it should be verified whether adhesions commonly form when an intact peritoneum is involved. In the study by Haney and Doty, adhesions were induced by injuring the medial aspects of murine uterine horns and approximating these tissues. The incidence of adhesions after injury on one side was compared with the incidence after injury on both sides, and the study found that the incidence was notably low after injury on one side.[13] The apparent difference between the hepatic model and the

uterine horn model indicates the need to investigate how frequently adhesions form after approximation of an injured tissue and an intact peritoneum under various conditions. Regarding gastrointestinal surgery, the effects of an injured tissue on the opposite intact peritoneum need to be clarified, particularly when injuries are caused at sites that are more relevant to intestinal obstructions, i.e. the intestine, mesentery, and parietal peritoneum.[41,42] Moreover, the effects should be investigated when injuries are caused by types of insults other than electrocautery including severe ischemia, which is presumed to be a potent stimulus for adhesion formation.[43,44] Any type of insult that frequently causes adhesions between an injured tissue and an intact peritoneum should be avoided in surgical procedures.

The possible role of MCs as a protective epithelium against adhesion formation advocates seeking an effective method of avoiding the detachment and injury of MCs and verifying whether the protection of MCs is associated with adhesion prevention. Prophylactic barrier materials have been developed and shown to be effective in preventing adhesions, yet more recent studies have

shown that commonly available materials are not sufficiently effective.[45,46] The results of the present study imply that protecting the MCs of the opposite intact peritoneum leads to the prevention of adhesion formation. However, not much has been reported on the effects of barrier materials on the MCs that lie beneath and in contact with these materials.[47] Barrier materials that maintain the epithelial integrity of MCs in contact with the materials and that are not biologically absorbed until the surface of an injured tissue is completely regenerated by MCs might be the most promising. In addition, the study by Haney and Doty has shown that two opposing injured tissues more frequently form adhesions than an injured tissue and an intact peritoneum, and the authors suggested that injuries to a normal peritoneum should be minimized wherever the peritoneum may come into contact with the main surgical site, where injuries are inevitable.[13] The results of the present study support this view in light of the protective role of MCs. Clarifying what manipulation of a peritoneum causes denudation of the peritoneum and seeking how to prevent the detachment of MCs may contribute to the prevention of adhesion formation.

A limitation of this study is that the methods of investigation are confined to morphological approaches, and an intervention in the model or the quantification of bioactive factors that could affect the function of MCs is needed to further clarify the underlying mechanisms. For example, the involvement of lubricants in the early detachment of MCs may be examined by detecting lubricants on the peritoneal surfaces and verifying whether applying exogenous lubricants, such as sialomucin or phosphatidylcholine, leads to a reduction in peritoneal denudation and the prevention of adhesions.[19,48.49] The effects of inflammatory cells on the opposite peritoneum at later stages can be investigated by quantifying inflammatory cytokines and verifying whether inhibiting these cytokines leads to the prevention of the morphological changes in MCs. In addition, more recent studies have shown that the factors released from necrotic tissues, i.e. damage-associated molecular patterns, cause sterile inflammation,[50,51] and the effects of these factors on MCs and their involvement in adhesion formation remain to be observed. These predicted mechanisms need to be verified in future studies.

In conclusion, the present study shows that an injured tissue affects the opposite intact peritoneum and forms adhesions with the opposite intact tissue. Further studies are needed to clarify the pathophysiology of adhesion formation after approximation of an injured tissue and an intact peritoneum. This study supports the significance of mesothelial cells as a protective barrier against adhesion formation and indicates that mesothelial cells can be a therapeutic target for the prevention of adhesion formation and the reduction of adhesion-related morbidity.

ACKNOWLEDGEMENTS

We thank Yoshiyasu Satake for animal care and surgical assistance, Satoshi Suzuki for maintenance of the electron microscope, Kouji Soman for checking the electrocautery device, and Dr. Yoshio Bando for providing technical advice on the preparation of cryosections. This study was supported by a generous

donation from Takeda Pharmaceutical Company Limited.

DISCLOSURE/CONFLICT OF INTEREST

This study was funded by Takeda Pharmaceutical Company Limited.

REFERENCE

1. Tingstedt B, Andersson E, Isaksson K, et al. Clinical impact of abdominal adhesions: what is the magnitude of the problem? Scand J Gastroenterol 2008;43:255-261.

2. Practice Committee of the American Society for Reproductive Medicine; Society of Reproductive Surgeons. Pathogenesis, consequences, and control of peritoneal adhesions in gynecologic surgery. Fertil Steril 2007;88:21-26.

3. Schnuriger B, Barmparas G, Branco BC, et al. Prevention of postoperative peritoneal adhesions: a review of the literature. Am J Surg 2011;201:111-121.

4. Holmdahl L. Making and covering of surgical footprints. Lancet 1999;353:1456-1457.

5. diZerega GS, Campeau JD. Peritoneal repair and post-surgical adhesion formation. Hum Reprod Update 2001;7:547-555.

6. Reed KL, Stucchi AF, Leeman SE, et al. Inhibitory Effects of a Neurokinin-1 Receptor Antagonist on Postoperative Peritoneal Adhesion Formation. Annals of the New York Academy of Sciences 2008;1144:116-126.

7. Kosaka H, Yoshimoto T, Yoshimoto T, et al. Interferon-γ is a therapeutic target molecule for prevention of postoperative adhesion formation. Nature Medicine 2008;14:437-441.

8. Tzianabos AO, Holsti MA, Zheng XX, et al. Functional Th1 cells are required for surgical adhesion formation in a murine model. J Immunol 2008;180:6970-6976.

9. Hellebrekers BW, Kooistra T. Pathogenesis of postoperative adhesion

formation. Br J Surg 2011;98(11):1503-1516.

10. Herrick SE, Mutsaers SE. Mesothelial progenitor cells and their potential in tissue engineering. Int J Biochem Cell Biol 2004;36:621-642.

11. Schade DS, Williamson JR. The pathogenesis of peritoneal adhesions: an ultrastructural study. Ann Surg 1968;167:500-510.

12. Lamont PM, Menzies D, Ellis H. Intra-abdominal adhesion formation between two adjacent deperitonealised surfaces. Surg Res Commun 1992;13:127-130.

13. Haney AF, Doty E. The formation of coalescing peritoneal adhesions requires injury to both contacting peritoneal surfaces. Fertil Steril 1994;61:767-775.

14. Martins PN, Neuhaus P. Surgical anatomy of the liver, hepatic vasculature and bile ducts in the rat. Liver Int 2007;27:384-392.

15. Namimatsu S, Ghazizadeh M, Sugisaki Y. Reversing the effects of formalin fixation with citraconic anhydride and heat: a universal antigen retrieval method. J Histochem Cytochem 2005;53:3-11.

16. Hilkens J, Ligtenberg MJ, Vos HL, et al. Cell membrane-associated mucins and their adhesion-modulating property. Trends Biochem Sci 1992;17:359-363.

17. Ohtsuka A, Yamana S, Murakami T. Localization of membrane-associated sialomucin on the free surface of mesothelial cells of the pleura, pericardium, and peritoneum. Histochem Cell Biol 1997;107:441-447.

18. Hills BA, Burke JR, Thomas K. Surfactant barrier lining peritoneal mesothelium: lubricant and release agent. Perit Dial Int 1998;18:157-165.

19. Bodega F, Pecchiari M, Sironi C, et al. Lubricating effect of sialomucin and hyaluronan on pleural mesothelium. Respir Physiol Neurobiol 2012;180:34-39.

20. Andreoli SP, Mallett C, Williams K, et al. Mechanisms of polymorphonuclear leukocyte mediated peritoneal mesothelial cell injury. Kidney Int 1994;46:1100-1109.

21. ten Raa S, van den Tol MP, Sluiter W, et al. The role of neutrophils and oxygen free radicals in post-operative adhesions. J Surg Res 2006;136:45-52.

22. Leak LV, Ferrans VJ, Cohen SR, et al. Animal model of acute pericarditis and its progression to pericardial fibrosis and adhesions: ultrastructural studies. Am J Anat 1987;180:373-390.

23. Jones M, Gabriel DA. Influence of the subendothelial basement membrane

components on fibrin assembly. Evidence for a fibrin binding site on type IV collagen. J Biol Chem 1988;263:7043-7048.

24. Wu C, Chung AE. Potential role of entactin in hemostasis. Specific interaction of entactin with fibrinogen A alpha and B beta chains. J Biol Chem 1991;266:18802-18807.

25. Tietze L, Borntraeger J, Klosterhalfen B, et al. Expression and function of β1 and β3 integrins of human mesothelial cells in vitro. Exp Mol Pathol 1999;66:131-139.

26. Laurens N, Koolwijk P, de Maat MP. Fibrin structure and wound healing. J Thromb Haemost 2006;4:932-939.

27. Stadlmann S, Raffeiner R, Amberger A, et al. Disruption of the integrity of human peritoneal mesothelium by interleukin-1β and tumor necrosis factor-α.

Virchows Archiv 2003;443:678-685.

28. Stadlmann S, Pollheimer J, Renner K, et al. Response of human peritoneal mesothelial cells to inflammatory injury is regulated by interleukin-1β and tumor necrosis factor-α. Wound Repair Regen 2006;14:187-194.

29. Jang YH, Shin HS, Sun Choi H, et al. Effects of dexamethasone on the TGF-β1-induced epithelial-to-mesenchymal transition in human peritoneal mesothelial cells. Lab Invest 2013;93:194-206.

30. Li Y, Wang J, Asahina K. Mesothelial cells give rise to hepatic stellate cells and myofibroblasts via mesothelial-mesenchymal transition in liver injury. Proc Natl Acad Sci U S A 2013;110:2324-2329.

31. Watters WB, Buck RC. Mitotic activity of peritoneum in contact with a regenerating area of peritoneum. Virchows Arch B Cell Pathol 1973;13:48-54.

32. Eskeland G, Kjaerheim A. Regeneration of parietal peritoneum in rats. 2. An electron microscopical study. Acta Pathol Microbiol Scand 1966;68:379-395.

33. Watters WB, Buck RC. Scanning electron microscopy of mesothelial regeneration in the rat. Lab Invest 1972;26:604-609.

34. Raftery AT. Regeneration of parietal and visceral peritoneum: an electron microscopical study. J Anat 1973;115:375-392.

35. Ryan GB, Grobety J, Majno G. Mesothelial injury and recovery. Am J Pathol 1973;71:93-112.

36. Whitaker D, Papadimitriou J. Mesothelial healing: morphological and kinetic investigations. J Pathol 1985;145:159-175.

37. Eming SA, Krieg T, Davidson JM. Inflammation in wound repair: molecular and cellular mechanisms. J Invest Dermatol. 2007;127:514-525.

38. Hinz B, Phan SH, Thannickal VJ, et al. The myofibroblast: one function, multiple origins. Am J Pathol 2007;170:1807-1816.

39. Bao P, Kodra A, Tomic-Canic M, et al. The role of vascular endothelial growth factor in wound healing. J Surg Res 2009;153:347-358.

40. Hoshino A, Kawamura YI, Yasuhara M, et al. Inhibition of CCL1-CCR8 interaction prevents aggregation of macrophages and development of peritoneal adhesions. J Immunol 2007;178:5296-5304.

41. Maetani S, Tobe T, Kashiwara S. Neglected role of torsion and constriction in pathogenesis of simple adhesive bowel obstruction. Br J Surg 1984;71:127-130.

42. Nieuwenhuijzen M, Reijnen MM, Kuijpers JH, et al. Small bowel obstruction after total or subtotal colectomy: a 10-year retrospective review. Br J Surg 1998;85:1242-1245.

43. Ellis H. The aetiology of post-operative abdominal adhesions. An experimental study. Br J Surg 1962;50:10-16.

44. Buckman RF Jr., Buckman PD, Hufnagel HV, et al. A physiologic basis for the adhesion-free healing of deperitonealized surfaces. J Surg Res 1976;21:67-76.

45. Rajab TK, Wallwiener M, Planck C, et al. A direct comparison of seprafilm, adept, intercoat, and spraygel for adhesion prophylaxis. J Surg Res 2010;161:246-249.

46. Shimizu A, Suhara T, Ito T, et al. A new hepatectomy-induced postoperative adhesion model in rats, and evaluation of the efficacy of anti-adhesion materials. Surg Today 2013 Epub ahead of print. DOI 10.1007/s00595-013-0530-8.

47. Haney AF, Doty E. Murine peritoneal injury and de novo adhesion formation caused by oxidized-regenerated cellulose (Interceed [TC7]) but not expanded polytetrafluoroethylene (Gore-Tex Surgical Membrane). Fertil Steril 1992;57:202-208.

48. Ar'Rajab A, Ahren B, Rozga J, et al. Phosphatidylcholine prevents postoperative peritoneal adhesions: an experimental study in the rat. J Surg Res 1991;50:212-215.

49. Snoj M, Ar'Rajab A, Ahren B, et al. Effect of phosphatidylcholine on postoperative adhesions after small bowel anastomosis in the rat. Br J Surg 1992;79:427-429.

50. McDonald B, Pittman K, Menezes GB, et al. Intravascular danger signals guide neutrophils to sites of sterile inflammation. Science 2010;330:362-366.

51. Kubes P, Mehal WZ. Sterile inflammation in the liver. Gastroenterology 2012;143:1158-1172.

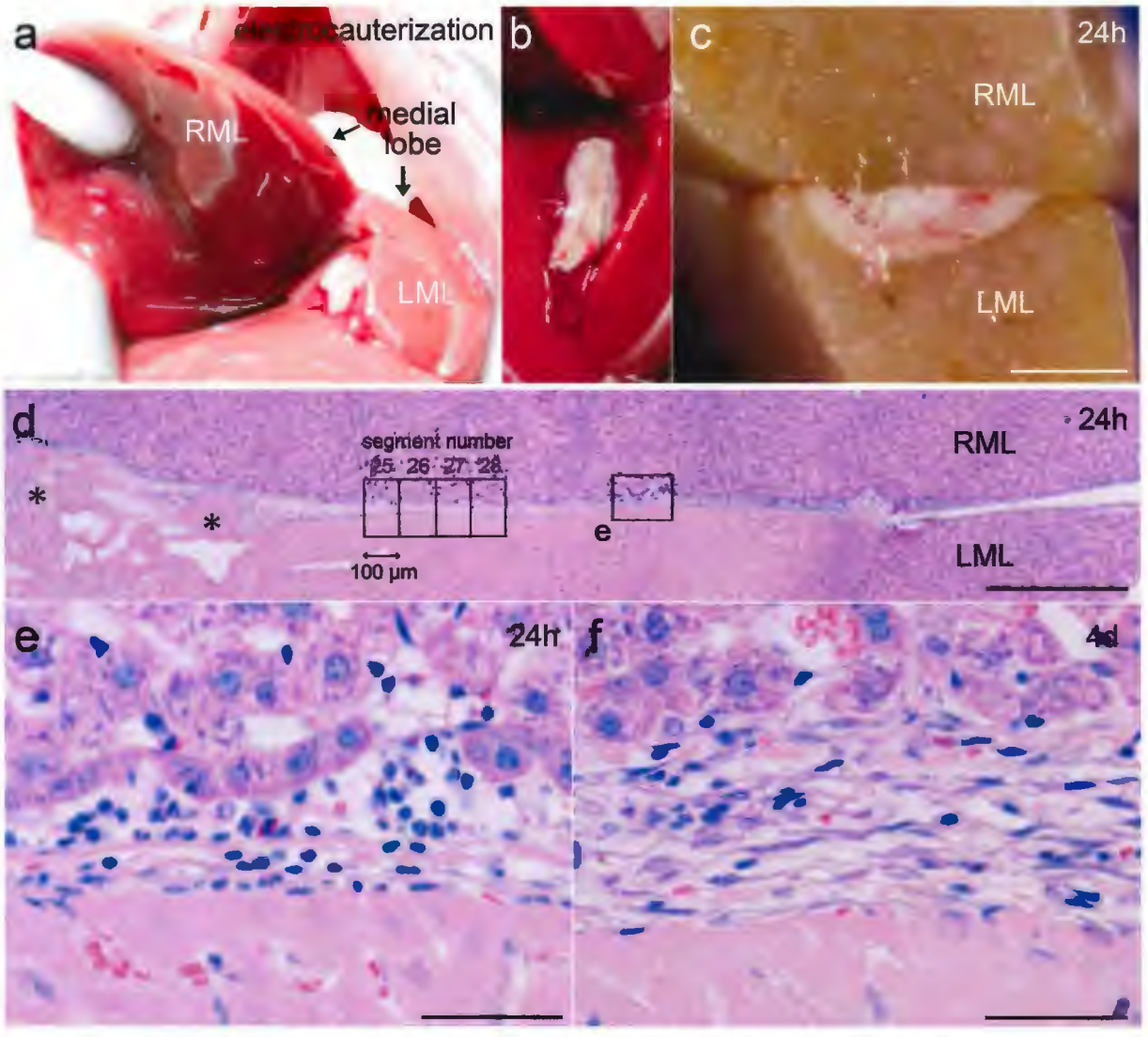

Figure 1 The hepatic model of adhesion formation. (a,b) Photographs of the liver at the time of electrocauterization. (c) A photograph showing a cross section of the excised liver at 24 hours after the procedure. Bar, 2 mm. (d) HE staining of the adherent lobes at 24 hours. An adhesion is seen over the necrotic hepatocytes, which are eosinophilic. The surface is uneven in the central part of the cauterized area (asterisks), where the tissue is deformed. Micrographs were divided into 100-μm-wide segments. Bar, 400 μm. (e) A closer view of (d). Mononuclear cells and polymorphonuclear leukocytes are seen in the adherent area. Bar, 40 μm. (f) At 4 days, flat cells and vessels are seen, forming granulation tissue. Bar, 40 μm. (g) The counts of the segments in which cauterized hepatocytes were necrotic are expressed as the mean + s.d. (n=6), whereas the counts of the segments in which the two lobes were adherent are shown in each value.

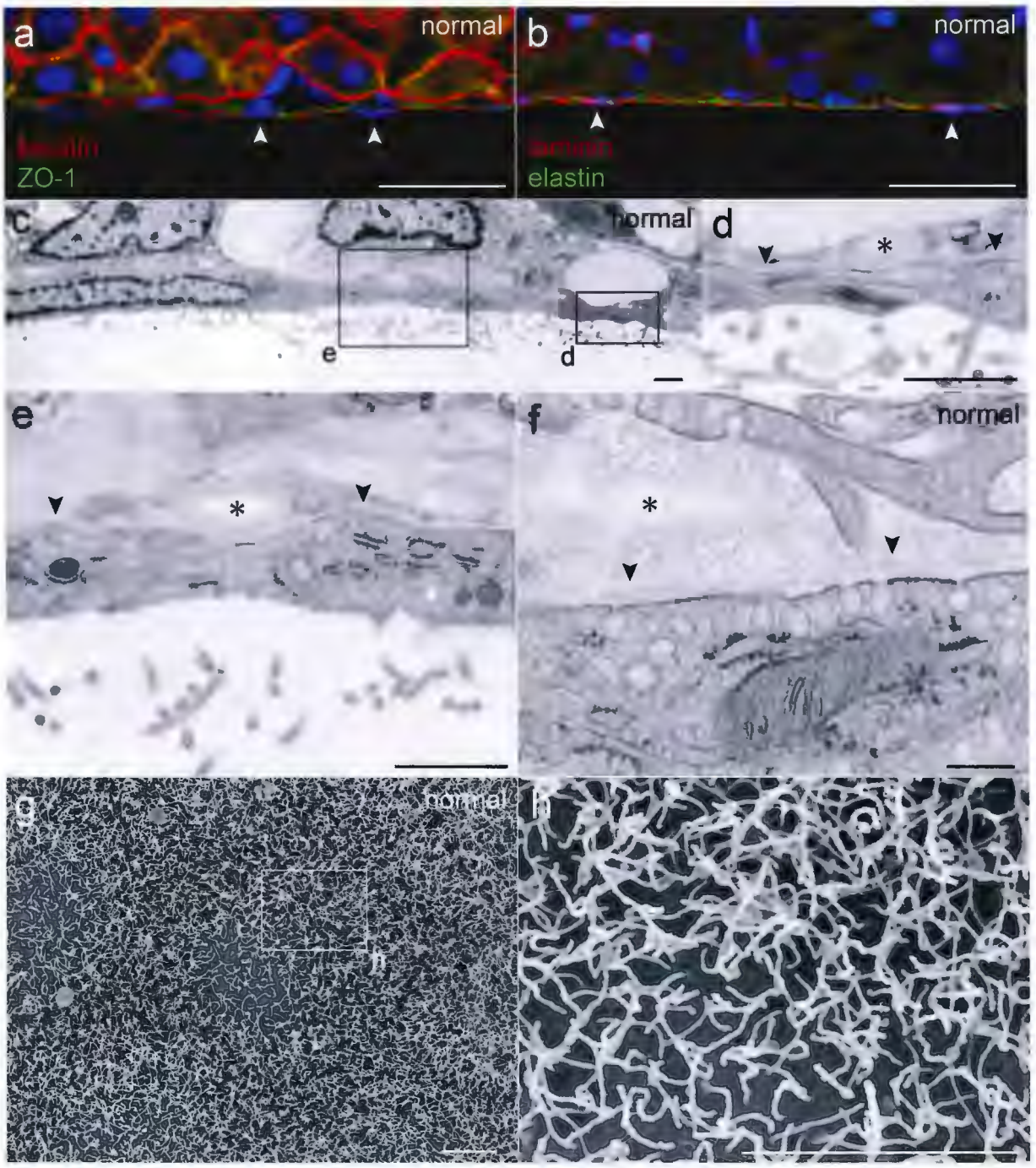

Figure 2 Normal liver peritoneum. (a,b) Immunohistochemical staining showing that MCs have keratin and ZO-1. A layer of laminin and elastin is seen beneath MCs. The nuclei of MCs (arrowheads) are indicated. Bar, 40 μm. (c-e) Micrographs of TEM showing flat MCs, a cell-cell junction and microvilli. The BM (arrowheads) and elastic fibers (asterisks) are indicated. Bar, 1 μm. (f) The BM is a thin layer of moderate electron density. The elastic fibers are electron-lucent with fine higher density at their periphery. A MC is shown in the lower part. Bar, 200 nm. (g,h) Micrographs of SEM showing the microvilli of MCs. Bar, 5 μm.

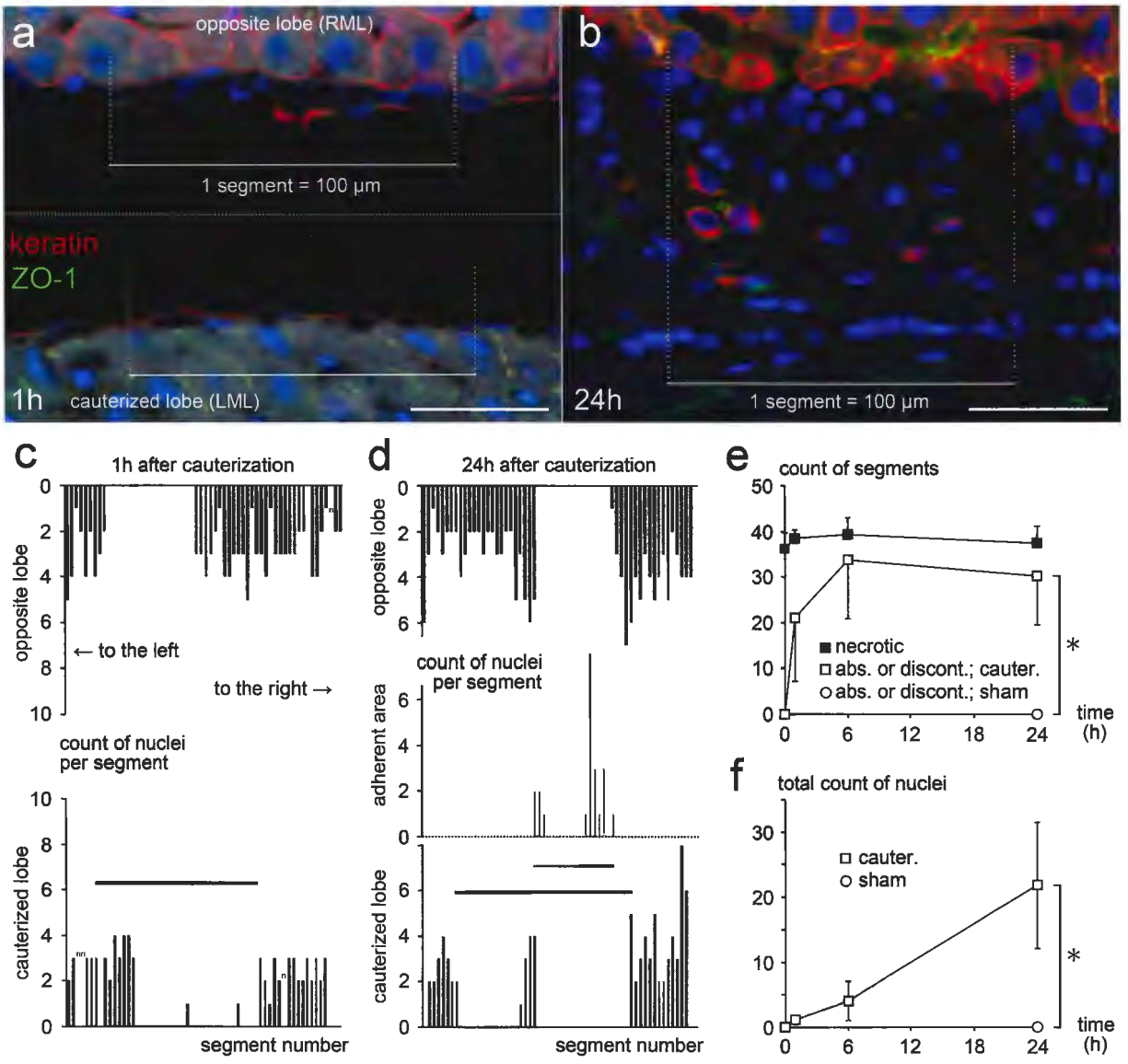

Figure 3 Distribution of MCs and their quantification. (a,b) Immunohistochemical staining for keratin and ZO-1 at 1 hour showing an edge of the denuded peritoneum, and at 24 hours showing a segment in which isolated MCs are remarkably seen in the adherent area. Bar, 40 μm. (c,d) Representative histograms of the counts of nuclei per segment at 1 hour and 24 hours. Black horizontal bars indicate the cauterized area, and gray bars indicate the adherent area, in which the isolated MCs were present. (e) The counts of the segments in which the MCs of the opposite lobe were absent or discontinuous (□after cauterization, ○after sham operation), and the counts of the segments in which hepatocytes of the cauterized lobe were necrotic (■) are shown. (f) The total counts of nuclei of the isolated MCs in the entire section. (e,f) The values at immediately after cauterization are shown at 0 hour. Values are expressed as the mean ± s.d. (n=4 at immediately after cauterization; n=6 at 1, 6 and 24 hours after cauterization; and n=3 at 24 hours after sham operation) ＊P<0.05 by Mann-Whitney's U test.

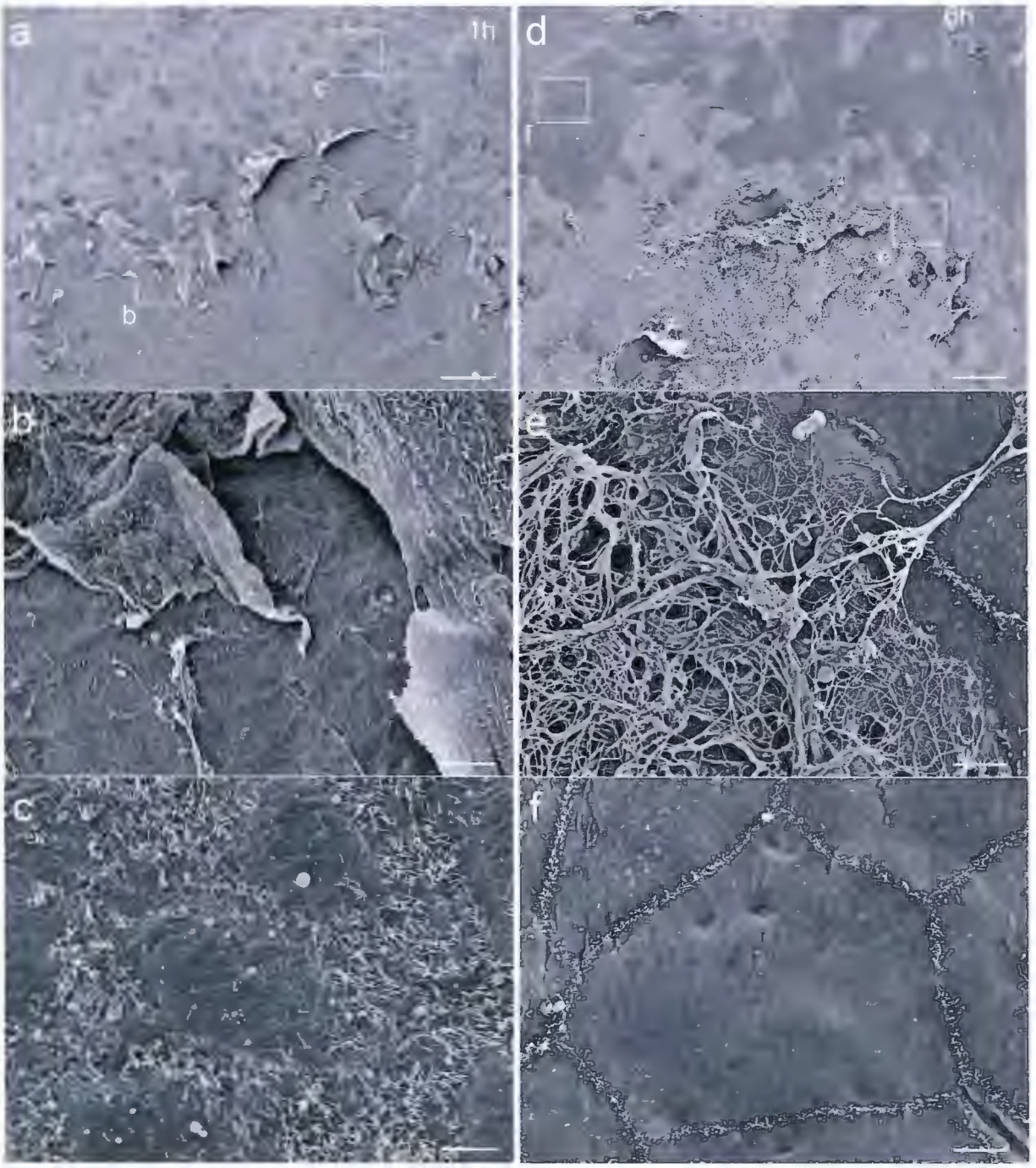

Figure 4 Observation of the opposite peritoneum by SEM. **(a-c)** At 1 hour, the opposite peritoneum has been denuded of MCs. The peritoneum is denuded abruptly at the margin, leaving a large island-shaped denuded area, where the underlying BM is exposed. The MCs at the margin are irregularly shaped. Microvilli are fewer in several of the MCs around the margin. (d-f) At 6 hours, fibrin fibers are seen over the denuded area. The irregularly shaped MCs are rarely seen at the margin. The MCs around the margin have much fewer and shorter microvilli. Bar, (a,d) 50 μm, (b,c,e,f) 5 μm.

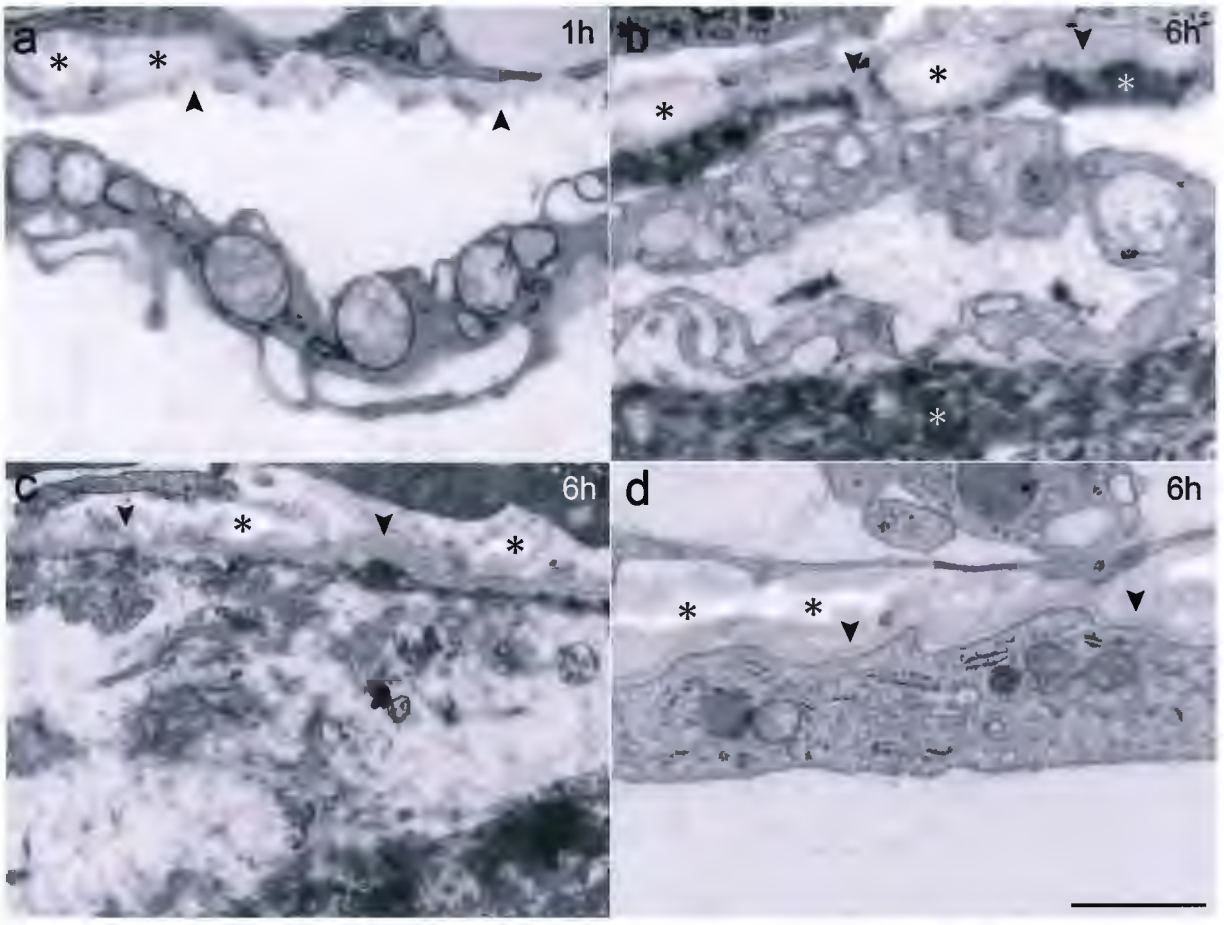

Figure 5 Observation of MCs of opposite peritoneum by TEM. (a) At the margin of the denuded area at 1 hour, irregularly shaped MCs possess swollen mitchondria and dilated rough endoplasmic reticulum. (b) In the denuded area at 6 hours, detached MCs with unrecognizable cytoplasmic organelles are occasionally seen. (c) In the denuded area at 6 hours, necrotic debris is also seen near the opposite peritoneum. (d) Around the margin at 6 hours, the MCs with diminished microvilli possess cytoplasmic organelles of normal appearance. (a-d) The BM (arrowheads), elastic fibers (black asterisks) and fibrin (white asterisks) are indicated. Bar, 1 μm.

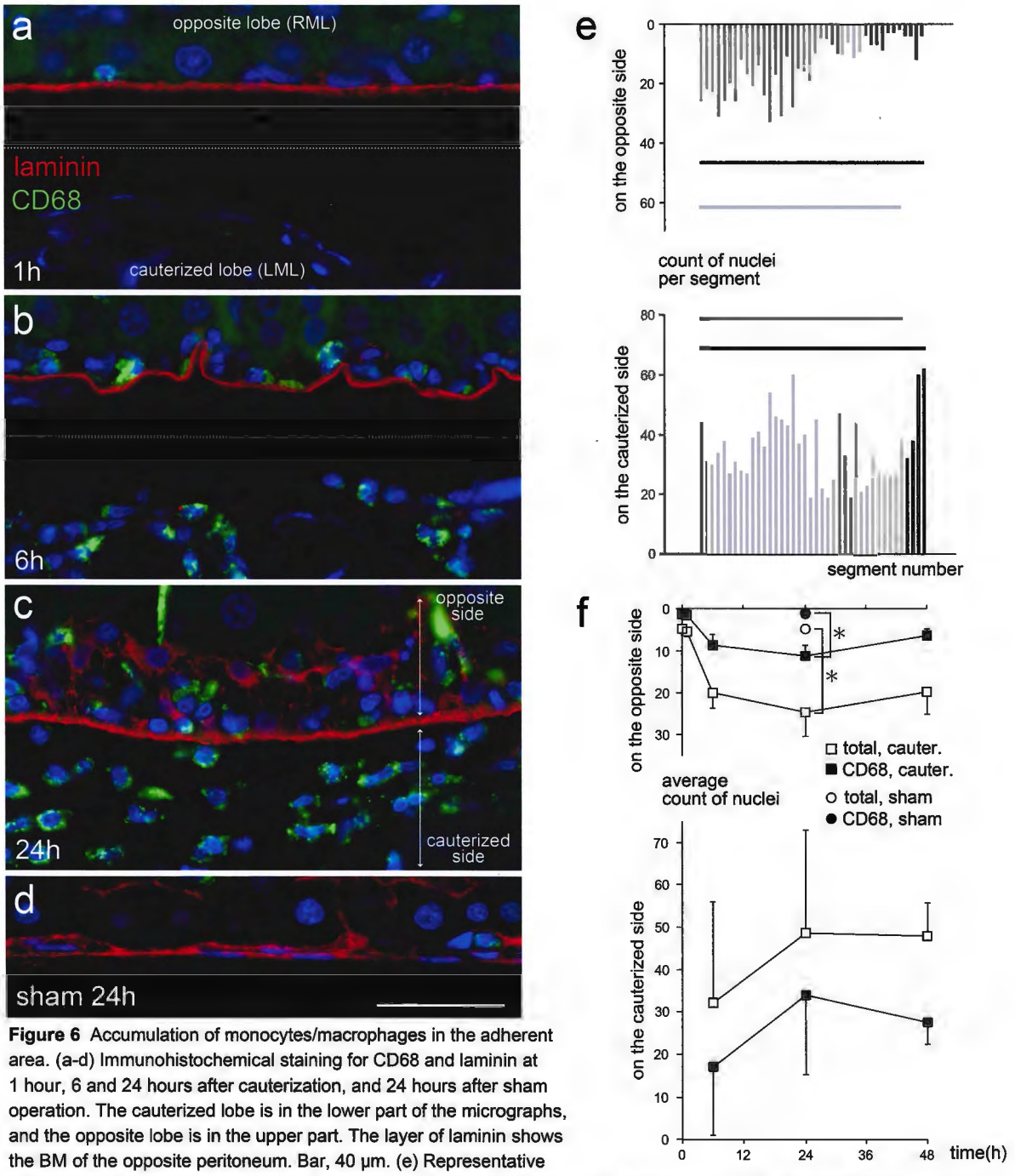

Figure 6 Accumulation of monocytes/macrophages in the adherent area. (a-d) Immunohistochemical staining for CD68 and laminin at 1 hour, 6 and 24 hours after cauterization, and 24 hours after sham operation. The cauterized lobe is in the lower part of the micrographs, and the opposite lobe is in the upper part. The layer of laminin shows the BM of the opposite peritoneum. Bar, 40 μm. (e) Representative histograms of the counts of nuclei per segment for CD68-positive cells at 24 hours showing the distribution of monocytes/ macrophages, on each side of the BM of the opposite peritoneum. Black horizontal bars indicate the cauterized area, and gray bars indicate the adherent area. (f) The average counts of nuclei per segment of total cells and CD68-positive cells in the cauterized area are expressed as the mean ± s.d. (n=3 for normal rats and 24 hours after sham operation, and n=4 at 1 hour, 6,24 and 48 hours after cauterization) ＊P<0.01 by a two sample t test with Welch's correction.

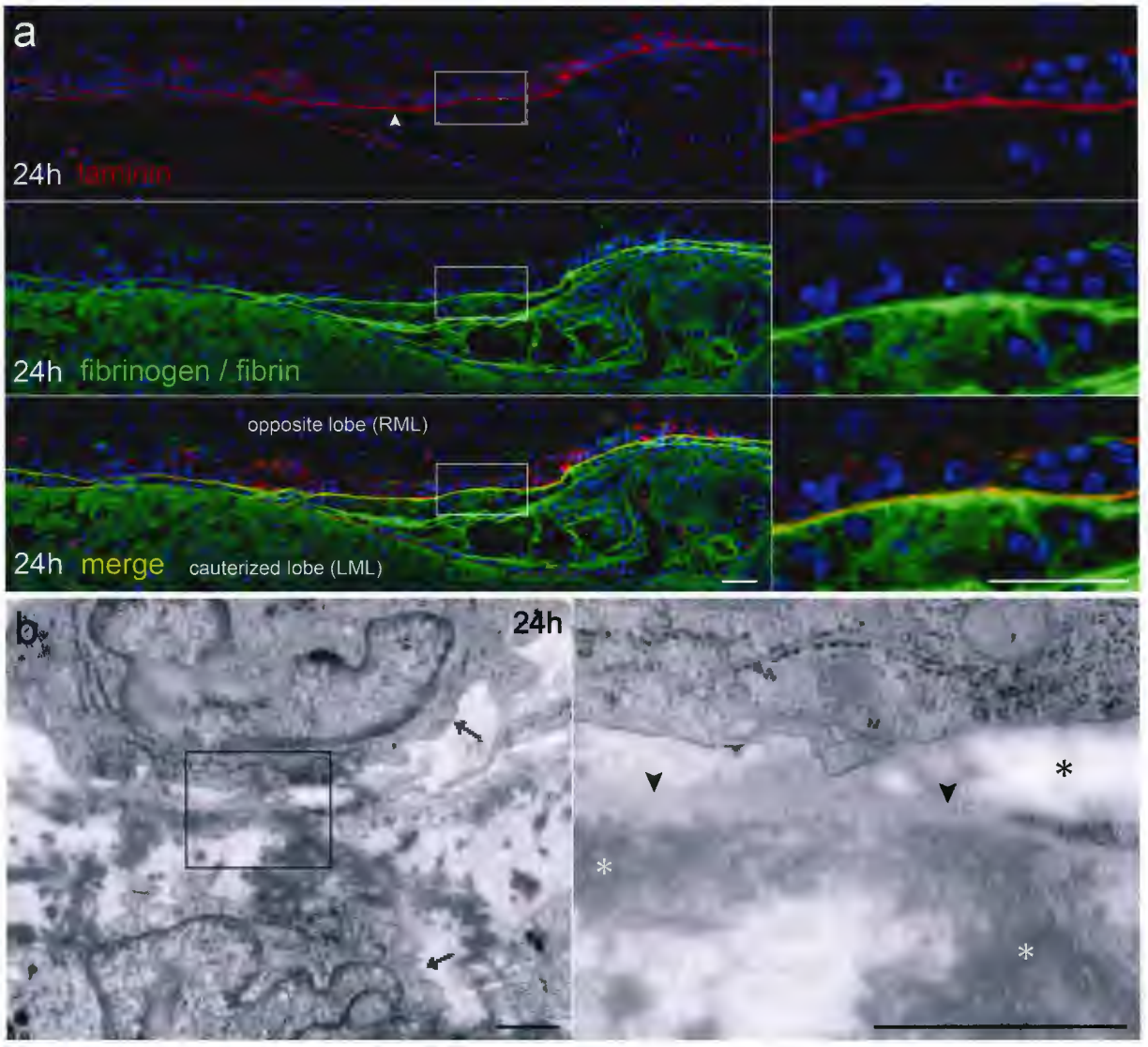

Figure 7 Fibrin attaches to the BM of the opposite peritoneum. (a) Immunohistochemical staining for laminin and fibrinogen/fibrin at 24 hours. The layer of laminin (arrowhead) indicates the BM of the opposite peritoneum. Fibrinogen/fibrin is extensively seen between the cauterized tissue and the BM of the opposite peritoneum, and in close proximity to the BM. Bar, 40 μm. (b) Micrographs of TEM at 24 hours. Fibrin (white asterisks) has attached to the BM (arrowheads) of the opposite peritoneum. The elastic fibers (black asterisk) are indicated. Macrophages (arrows) are seen on each side of the BM. Bar, 1 μm.

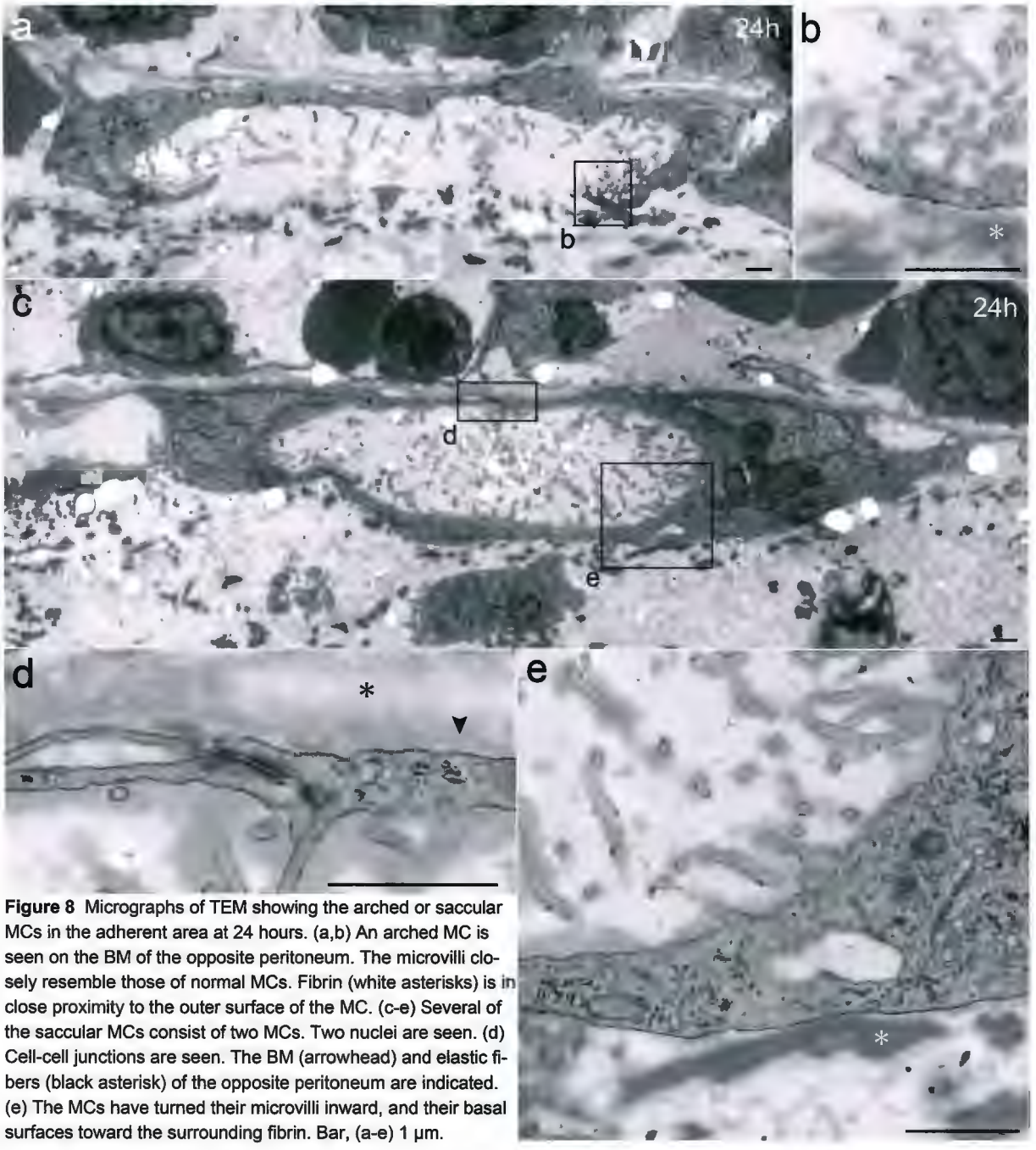

Figure 8 Micrographs of TEM showing the arched or saccular MCs in the adherent area at 24 hours. (a,b) An arched MC is seen on the BM of the opposite peritoneum. The microvilli closely resemble those of normal MCs. Fibrin (white asterisks) is in close proximity to the outer surface of the MC. (c-e) Several of the saccular MCs consist of two MCs. Two nuclei are seen. (d) Cell-cell junctions are seen. The BM (arrowhead) and elastic fibers (black asterisk) of the opposite peritoneum are indicated. (e) The MCs have turned their microvilli inward, and their basal surfaces toward the surrounding fibrin. Bar, (a-e) 1 μm.

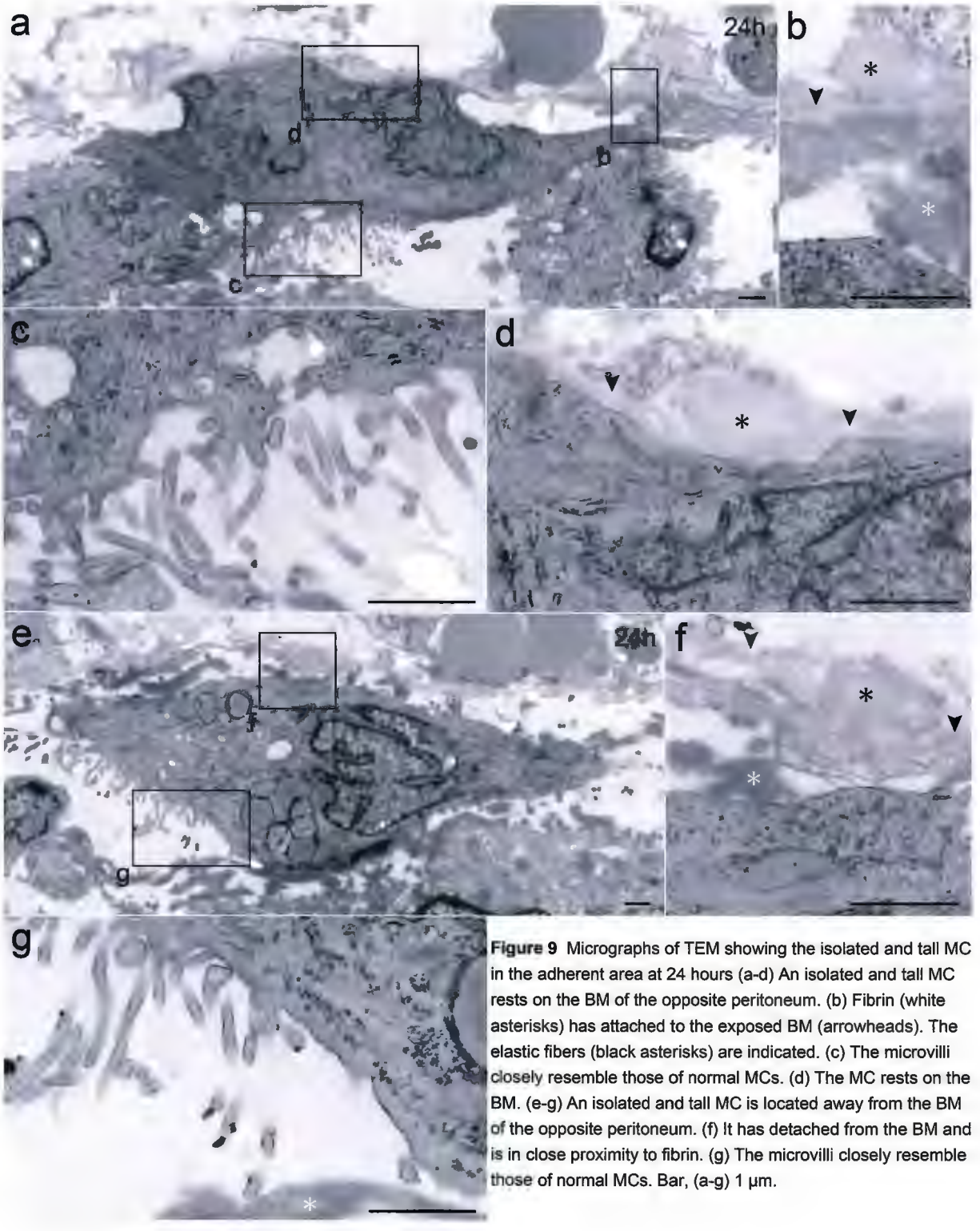

Figure 9 Micrographs of TEM showing the isolated and tall MC in the adherent area at 24 hours (a-d) An isolated and tall MC rests on the BM of the opposite peritoneum. (b) Fibrin (white asterisks) has attached to the exposed BM (arrowheads). The elastic fibers (black asterisks) are indicated. (c) The microvilli closely resemble those of normal MCs. (d) The MC rests on the BM. (e-g) An isolated and tall MC is located away from the BM of the opposite peritoneum. (f) It has detached from the BM and is in close proximity to fibrin. (g) The microvilli closely resemble those of normal MCs. Bar, (a-g) 1 μm.

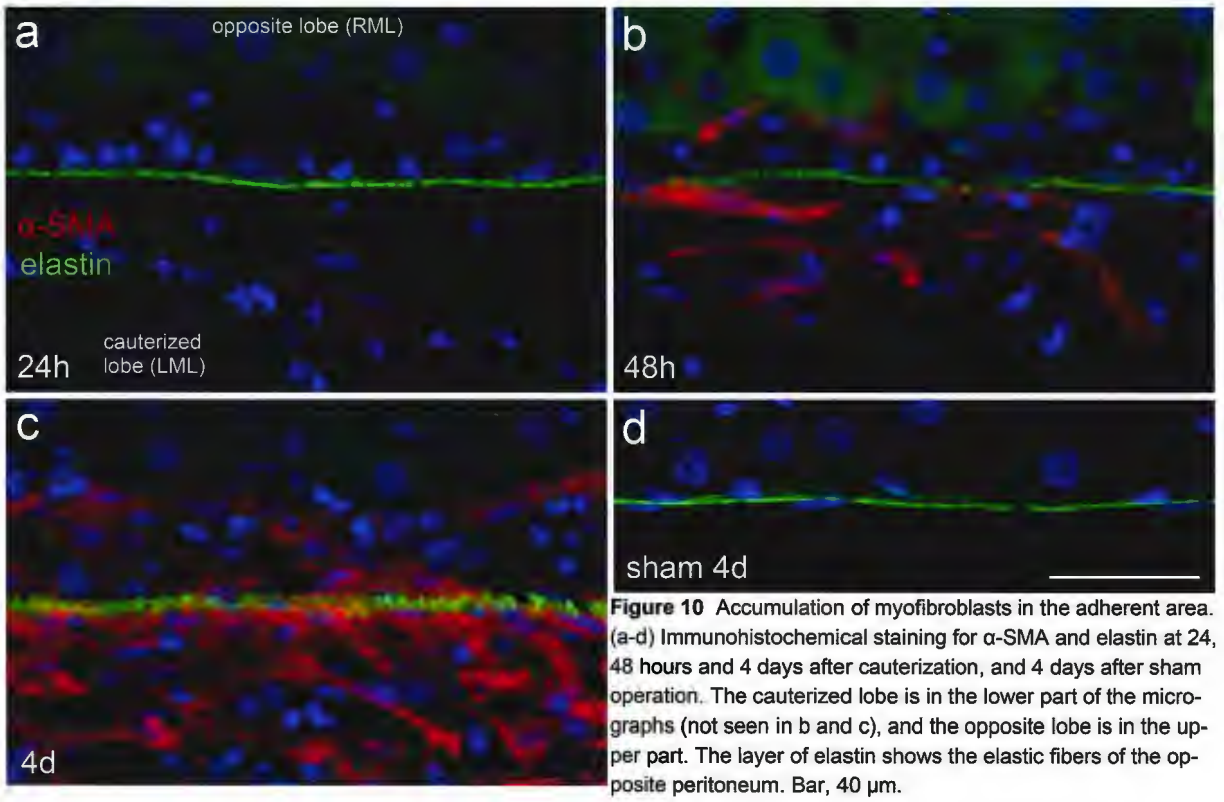

Figure 10 Accumulation of myofibroblasts in the adherent area. (a-d) Immunohistochemical staining for α-SMA and elastin at 24, 48 hours and 4 days after cauterization, and 4 days after sham operation. The cauterized lobe is in the lower part of the micrographs (not seen in b and c), and the opposite lobe is in the upper part. The layer of elastin shows the elastic fibers of the opposite peritoneum. Bar, 40 μm.

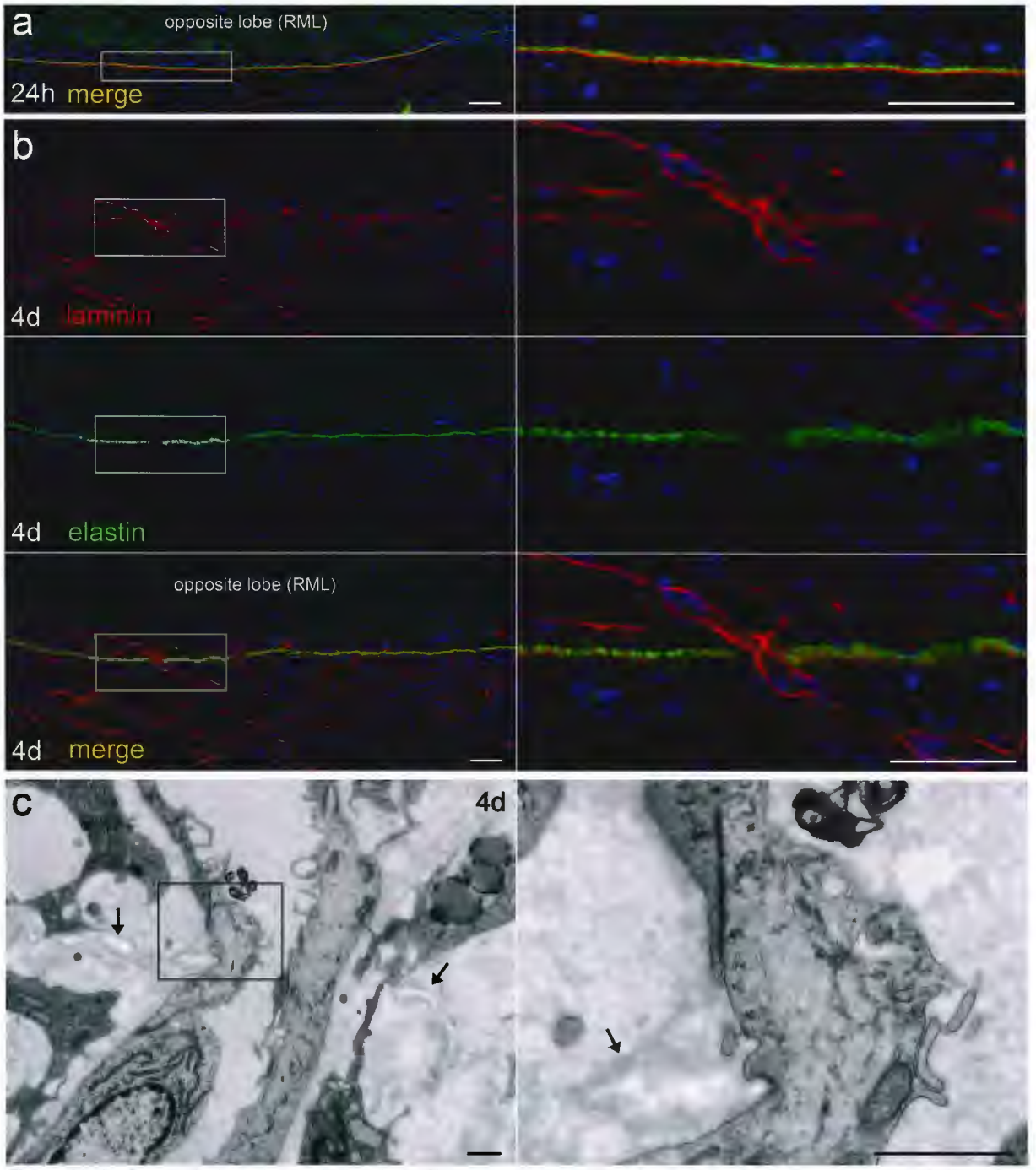

Figure 11 Angiogenesis through gaps in the elastic fibers. (a,b) Immunohistochemical staining for laminin-γ1 and elastin at 24 hours and 4 days. A layer of the BM and elastic fibers of the opposite peritoneum is shown at 24 hours. At 4 days, new layers of BM have appeared, forming lumen-like structures. The newly formed BM has grown through gaps of the elastic fibers of the opposite peritoneum. Bar, 40 μm. (c) Micrographs of TEM at 4 days showing that a newly formed vessel consisting of endothelial cells with cell-cell junctions has grown through a gap of the elastic fibers (arrows) of the opposite peritoneum. Bar, 1 μm.

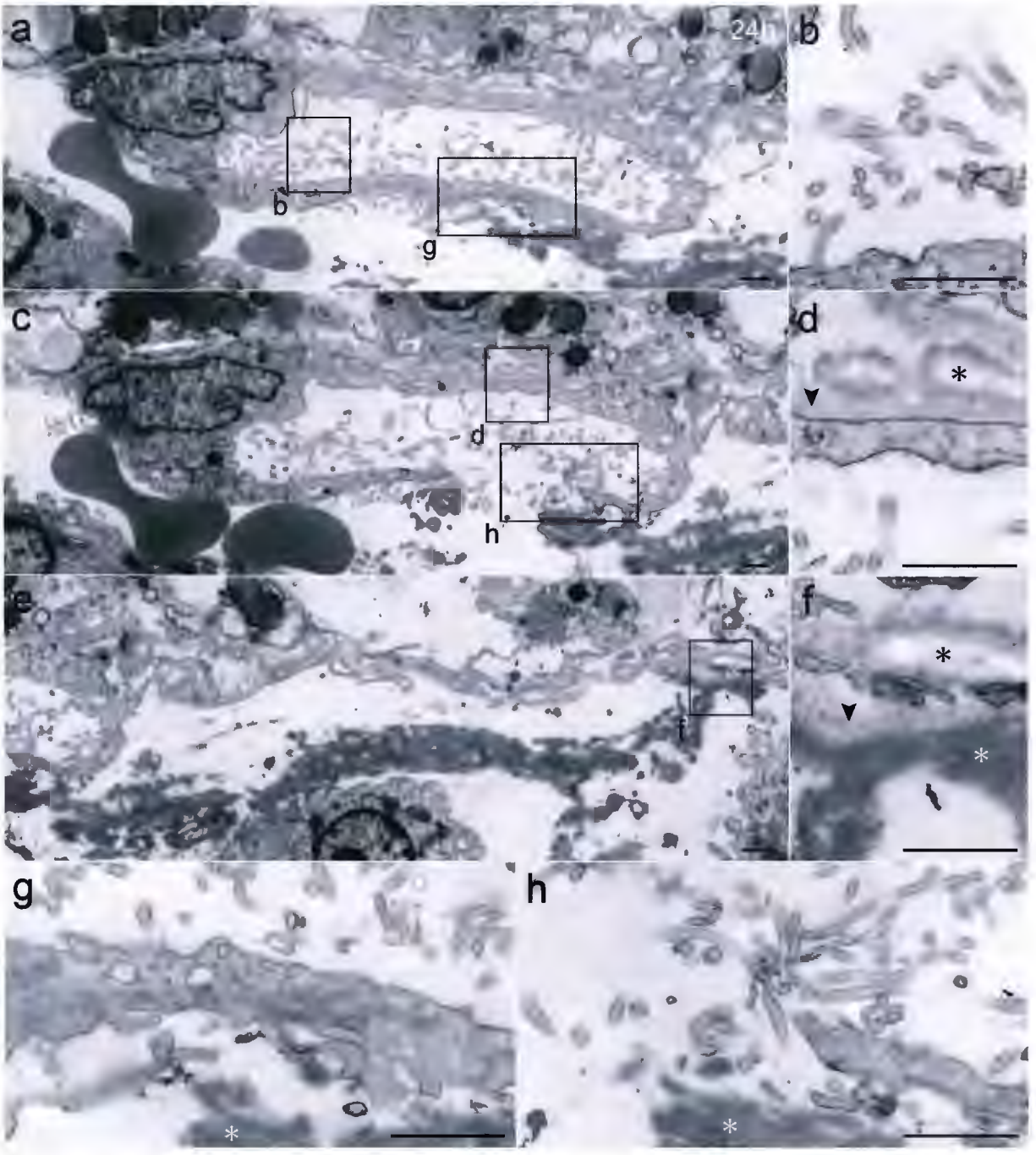

Supplementary Figure 1 Micrographs of TEM showing a single saccular MC in the adherent area at 24 hours. (**a**,**b**,**g**) Observation of a section shows no apparent gaps or cell-cell junctions in the saccular MC. (**c**,**d**,**h**) Another section of the same cell shows that the saccular space is not totally closed. (**e**,**f**) On the right side of the figure (c), fibrin has attached to the exposed BM. Fibrin (white asterisks), BM (arrowheads) and elastic fibers (black asterisks) of the opposite peritoneal surface are indicated. Bar, (**a**-**h**) 1 μm.

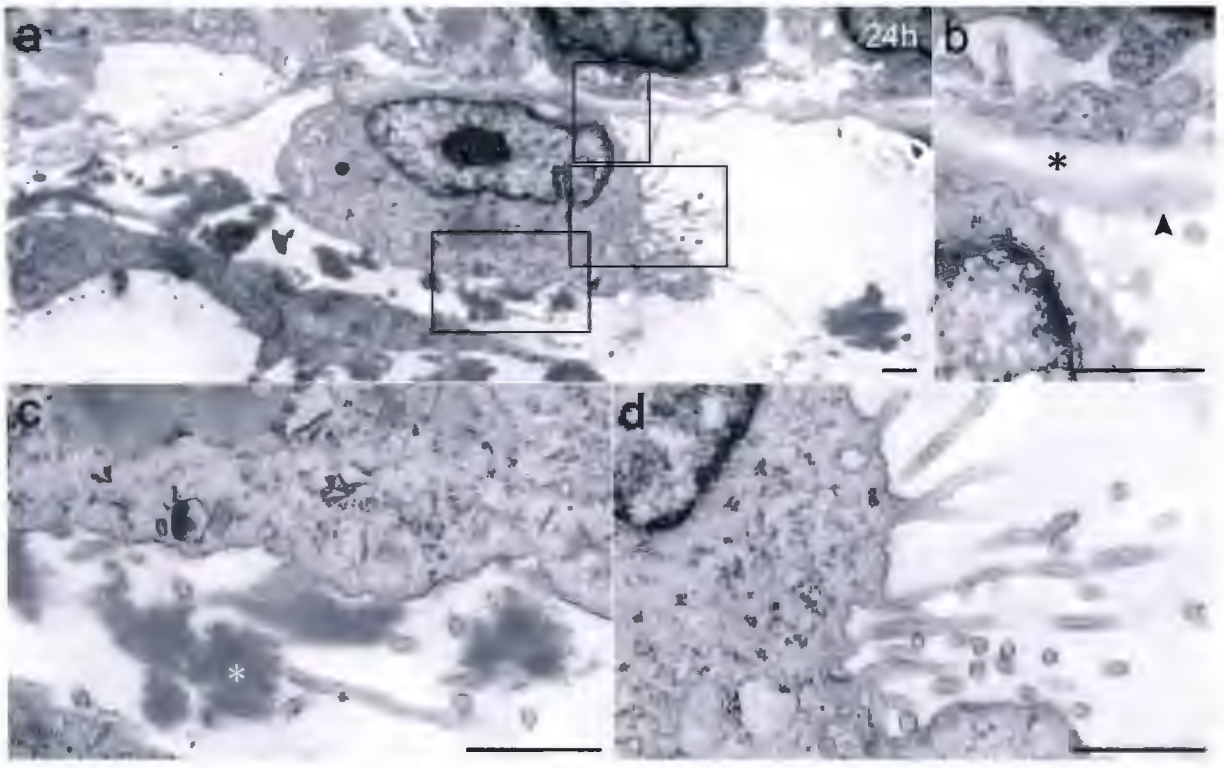

Supplementary Figure 2 Micrographs of TEM showing an isolated and tall MC at 24 hours after cauterization. (**a**) The MC is located on the BM of the opposite peritoneum and on fibrin at the same time. (**b**) The BM (arrowhead) and elastic fibers (black asterisk) are indicated. (**c**) The MC is in close proximity to fibrin (white asterisk). (**d**) The microvilli closely resemble those of normal MCs. Bar, (**a-d**) 1 μm.

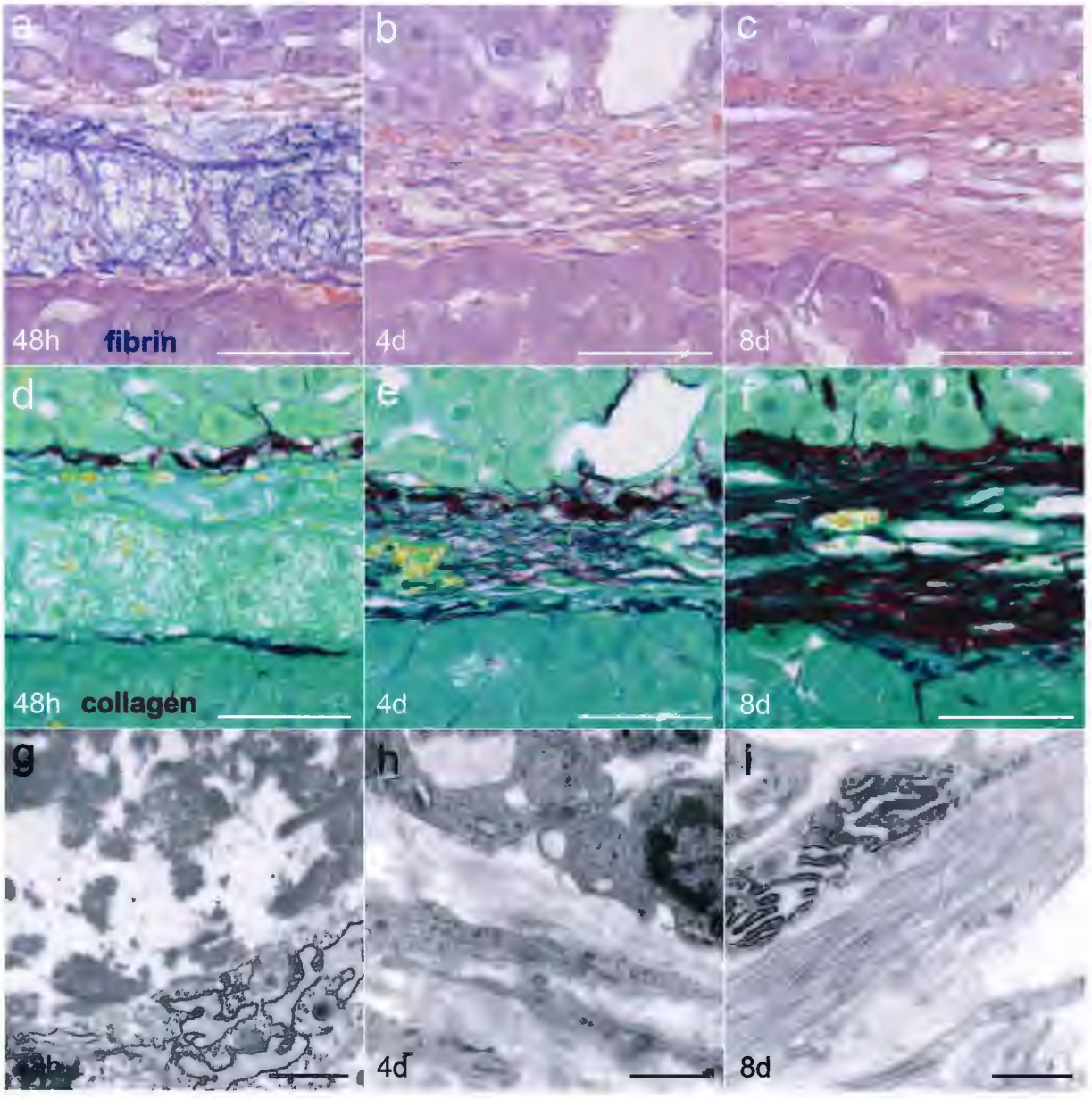

Supplementary Figure 3 Fibrin is replaced by collagen. (a-c) Phosphotungstic acid hematoxylin staining, (d-f) Sirius red and Fast Green staining, (g-i) TEM, (a,d,g) at 48 hours, (b,e,h) at 4 days, (c,f,i) at 8 days. Fibrin fibers are dyed blue by phosphotungstic acid hematoxylin staining, and collagen fibers are dyed red by Sirius red and Fast Green staining. Micrographs of TEM show fibrin fibers at 48 hours, collagen fibrils at 4 days, and thicker collagen bundles at 8 days. Bar, (a-f) 40 μm, (g-i) 1 μm.